

Chapter 7

Genomic integration of *E. coli* NADH insensitive *cs* and *Salmonella typhimurium* Na⁺ dependent citrate transporter with *vgb*, *egfp* in *B. japonicum* USDA110 *M. loti* MAFF030669 and *S. fredii* NGR 234

7.1 Introduction

Inoculation of microbial consortium of P solubilizing *Bacillus megaterium* and N fixing free bacteria like *Azotobacter* have been found to be more effective than individual members (Aditya et al., 2009). In field experiments, *Penicillium bilaii* and *Bacillus megatherium* are known to be most effective phosphate solubilizing microorganisms (PSMs) (Asea et al., 1988; Kucey, 1988).

Overexpression of *ppc* gene of *S. elongatus* in *B. japonicum* USDA110 and *M. loti* MAFF030669 enhanced cellular biomass, glucose catabolism through intracellular phosphorylative pathway and resulted in increase in gluconic acid and citric acid secretion, which was due to increased activities of both PYC and PPC. Similar levels of citric acid secretion was seen upon overexpression of wild type *cs* gene but there was a decrease in P solubilization compared to *ppc* gene overexpression which may be attributed to lower levels of gluconic acid secretion in *cs* overexpression. Additionally, overexpression of *E. coli* NADH insensitive *cs* gene in *B. japonicum* USDA110 and *M. loti* MAFF030669 strains also resulted in minor increase in secretion of citric acid but P solubilization showed a significant improved phenotype which is correlated with ~ 2.6 fold increase in gluconic acid secretion. The gluconic acid secretion was more than even *ppc* overexpression. Interestingly, overexpression of citrate transporter along with NADH insensitive *cs* gene increased citric secretion upto ~10 mM citric acid and gluconic acid level remained high which further enhanced MPS phenotype. Earlier studies showed that 10 mM citric and 20 mM gluconic acids released 0.7 mM and 0.5 mM P from alkaline vertisols, respectively (Gyaneshwar et al., 1998). Thus, the *B. japonicum* USDA110 and *M. loti* MAFF030669 transformants containing NADH insensitive *cs* and *citC* genes could be effective PSMs in alkaline vertisols.

Presence of plasmids adversely affected the growth and gluconic acid secretion of phosphate solubilizing *Enterobacter asburiae* PSI3 under phosphorus limited condition (Sharma et al. 2011). Similarly, *Azotobacter vinelandii*, *Azospirillum brasilense*, and *Pseudomonas putida* GR12-2 also showed impaired growth, phosphate solubilization, nitrogen fixation, siderophore production, and indole acetic acid biosynthesis, under various experimental conditions (Glick 1995). The maintenance of plasmid DNA in *E. coli* has been demonstrated to have diverse effects on the physiology and cellular metabolism including alteration in ATP biosynthesis as well as perturbations in host DNA replication, transcription, and translation (Rozkov et al. 2004; Wang et al. 2006; Chou 2007; Ow et al. 2006; 2009). Presence of *colE1* based plasmid has been demonstrated to significantly alter several metabolic pathways in *E. coli* depending on the growth conditions. Additionally, plasmids are not very stable in natural soil isolates and presence of antibiotic marker also impose problem in field conditions (De Gelder, 2007; Buch et al., 2010). Presence of plasmid affects the host metabolism adversely which results in different metabolic perturbations including alterations of several metabolic pathways in *E. coli* depending on the growth conditions due the presence of *colE1* based plasmid (Wang et al. 2006). Variable stability of *P. fluorescens* WCS365 and reduction in competitiveness of *P. putida* GR12-2 were found under rhizospheric conditions (Simons et al. 1996; Schmidt-Eisenlohr et al., 2003).

Previous reports from our laboratory showed that presence of plasmids and overexpression of genes in plasmids exerted greater metabolic alterations on *P. fluorescens* ATCC 13525 metabolism despite of low copy number (Buch et al., 2010). Thus to minimize the plasmid load, instability and antibiotic marker free genetic manipulation an artificial citrate gene cluster consisting NADH insensitive citrate synthase (*cs**), sodium dependent citrate transporter (*citC*), *Vitreoscilla hemoglobin* (*vgb*) and *egfp* were integrated into the genome of *B. japonicum* USDA110, *M. loti* MAFF030669 and *S. fredii* NGR234 by miniTn7 based integration system at *att* site and characterized the biochemical, growth and MPS abilities.

The mini-Tn7 transposon is very effective for single copy tagging of bacteria in a site-specific manner at a unique and neutral site without any deleterious effects. The Tn7 transposon was originally discovered by Barth et al. (1976) on the plasmid R483 (IncI α) as an element carrying the resistance genes trimethoprim (TmR) and streptomycin/spectinomycin (SmR/ SpR), which could be transposed to other replicons. These genes are flanked by the ends of the transposon, named the left (Tn7L) and the right (Tn7R) end (Lichtenstein and Brenner, 1982; Rogers et al., 1986). The Tn7 transposition process has been studied intensively in *E. coli* in which Tn7 inserts with high efficiency and unique orientation into one specific location named the attTn7 site (Peters et al., 2001). This site of insertion is located just downstream of the coding region, in the transcriptional terminator, of the *glmS* gene and thereby does not disrupt the gene (Gringauz, et al., 1988). The *glmS* gene encodes a glucosamine synthetase, which is required for cell wall synthesis (Vogler et al., 1989). It is conserved among many bacteria and therefore Tn7 is likely to have the same specific insertion site in many different bacteria, some have already been tested. The transposon genes required for specific insertion into the attTn7 site, are *tnsABCD*, and they function in *trans*. Thus, sequences located in the 3' end of the coding region of *glmS* are recognised by transposase proteins directing the actual insertion into the attTn7 site, down-stream of the *glmS* gene. However, if this site is unavailable the transposon can insert into other sites with low frequency.

The mini-Tn7-based gene integration system has been used for gene complementation, gene expression analysis, strain construction, and reporter gene-tagging of *Pseudomonas aeruginosa* and *Yersinia pestis*, particularly in biofilm and animal models. Heterologous genes including *lacZ* (β -galactosidase), *est* (esterase), and *gfp* (green fluorescent protein) under the control of the methanol dehydrogenase promoter have been integrated into the intergenic region between *glmS* and *dhaT* via the delivery of mini-Tn7 in *Methylobacterium extorquens*. A gene encoding for different fluorescent protein and luciferase protein along with promoter was integrated into the chromosomes of *Erwinia chrysanthemi*, *P. fluorescens*, *Pseudomonas syringae*, *P. putida* and many gram negative bacteria by the Tn7-based delivery system (Koch et al., 2001, Lambersten

et al., 2004; Choi et al., 2008). This gene delivery system was also applied to other organisms, such as *Burkholderia* spp. and *Proteus mirabilis*, which were determined to have multiple *glmS*-linked attTn7 sites and secondary, non-*glmS*-linked attTn7 site, respectively. Thus mini Tn7 transposition is a powerful technique for the integration or excision of a gene of interest at a single-copy on the chromosomal level, which makes it possible to conduct a variety of experiments, including insertional random mutagenesis, gene expression analysis, protein functional studies, or the gene-tagging of bacteria in living organisms.

MPS ability of the bacterial transformants in field conditions could be affected by various parameters. In addition to the nutrient availability and soil properties, oxygen limitation could be a significant factor. Oxygen is present in limited amounts in the rhizosphere which could limit the colonization and survival of rhizobacteria (Ramírez et al., 1999). Genetically modified *Rhizobium* with *vgb* overexpression has enhanced the growth of *Rhizobium* and also increased nitrogen content in bean plants (Ramírez et al., 1999).

The present study describes the genomic integration of *E. coli* NADH insensitive *cs* Y145F along with *S. typhimurium* sodium citrate transporter *citC* gene, *vhb* gene and *egfp* into *Rhizobium* genome of *B. japonicum* USDA110, *M. loti* MAFF030669 and *S. fredii* NGR234 and compare its effect to plasmid based expression on glucose catabolism and citric acid secretion.

7.2 Experimental design

7.2.1: Bacterial strains used in this study

Table 7.1: Bacterial strains used in this study. The details of the plasmids and the concentration of the antibiotics used are given in the **Table 2.2** and **2.3**.

Plasmid/Strains	Characteristics	Source or Reference
pGRG36	Intergration vector (Tn7)	Gregory et al., 2006
pUCPM18	pUC18 derived Broad-Host-Range vector; Ap ^r	Hester et al., 2000
<i>E. coli</i> DH10B	<i>Str^r F endA1 recA1 galE15 galK16 nupG rpsL ΔlacX74 Φ80lacZ ΔM15 araD139 Δ(ara,leu)7697 mcrA Δ(mrr-hsdRMS-mcrBC) λ</i>	(Invitrogen) USA
pJNK4	pUCPM18 with <i>E. coli</i> NADH insensitive <i>cs</i> * gene citrate transporter <i>citC</i> of <i>Salmonella typhimurium</i> under <i>Plac</i> and <i>km^r</i> gene; Ap ^r , Km ^r	Wagh, 2013
pJIYC	pGRG36 with with <i>E. coli</i> NADH insensitive <i>cs</i> * gene citrate transporter <i>citC</i> of <i>Salmonella typhimurium</i> under <i>Plac</i> , <i>vgb</i> gene and <i>egf</i> gene Ap ^r	This study
<i>Bj</i> intYc	Genomic integrant of <i>B. japonicum</i> USDA110 containing <i>lac-YF citC</i> , <i>vgb</i> , <i>egfp</i> Ap ^r	This study
<i>Ml</i> intYc	Genomic integrant of <i>M. loti</i> MAFF030669 containing <i>lac-YF citC</i> , <i>vgb</i> , <i>egfp</i> Ap ^r	This study
<i>Sf</i> intYc	Genomic integrant of <i>S. fredii</i> NGR234 containing <i>lac-YF citC</i> , <i>vgb</i> , <i>egfp</i> Ap ^r	This study

7.2.2: Cloning of artificial citrate operon in integration vector.

Construction of artificial citrate operon containing constitutive *lac* promoter, NADH insensitive citrate synthase (*cs**), Na⁺ dependent citrate transporter (*citC*), *vhb* gene and *gfp* was done as per the following strategy. XT-20 polymerase was used for PCR amplification (Bangalore Genei, India) from plasmid pJNK4. Sequence of forward (*lac*) primer 5' TCCGAAATGTGAAATACGAAGGCCGAGCATACAACACACAGGAGG ACGCATGATGGCTGATACAAAAGC 3' and reverse primer of *citC* gene 5' TTACACCATCATGCTGAACACGATGC 3' was used to amplify artificial citrate operon. Plasmid pGRG36-mini-Tn7-Amp-*egfp* was digested with *Sma*I, gel purified and ligated with 2.9 kb amplicon containing artificial citrate operon was ligated with pGRG36 containing *vgb* and *egfp* (Fig. 7.1). Clone was confirmed by restriction digestion and PCR amplification. Resultant construct of 17.9 kb, named as pJIYC consisted of artificial citrate operon.

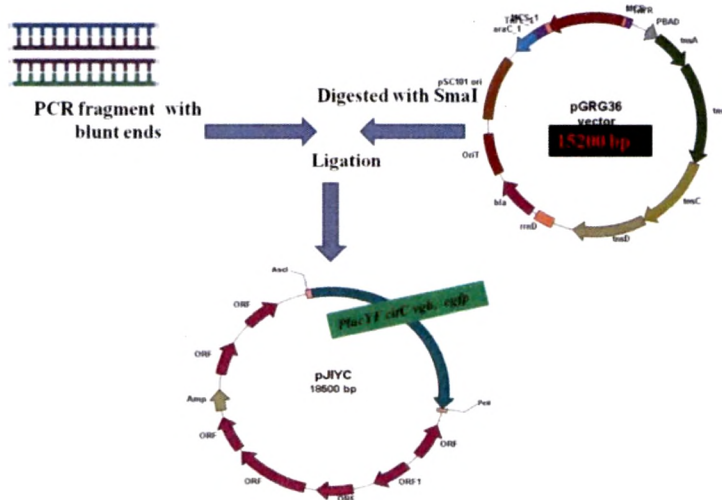


Fig. 7.1: Strategy used for cloning of artificial citrate operon in pGRG36 containing *vhb*, *egfp* resulted in pJIYC.

7.3: RESULTS

7.3.1: Construction of Genome integrants of *B. japonicum* USDA110 *M. loti* MAFF030669 and *S. fredii* NGR234

PCR amplification of NADH insensitive citrate synthase (*cs*^{*}) along with *citC* gene- Na⁺ dependent transporter under constitutive *lac* promoter was done from pJNK4 plasmid containing YF*citC* by using specific primers as mentioned above. This PCR amplicon was used for ligation with integration vector (**Fig.7.2**). For further confirmation, the recombinant plasmid pJIYC plasmid containing NADH insensitive Y145F and *S. typhimurium* sodium citrate transporter operon under constitutive *lac* promoter was confirmed by restriction enzyme digestion. pJIYC was digested with PvuII and pGRG36*vhb*, *egfp* plasmid digested with PvuII (**Fig. 7.3**).

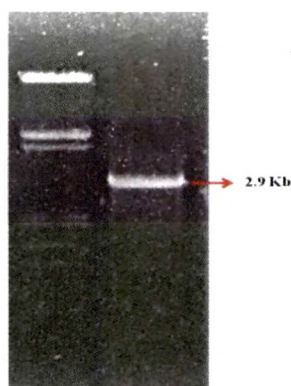


Fig. 7.2: PCR amplification of YF*citC* with constitutive *lac* promoter

Lane1- Marker HindIII/EcoRI, Lane2- PCR amplification with constitutive *lac* promoter

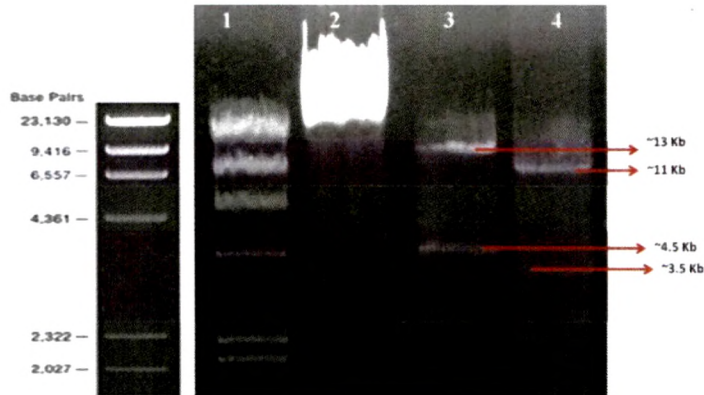


Fig.7.3: Restriction enzyme digestion pattern of pJIYC plasmid containing NADH insensitive Y145F and *S. typhimurium* sodium citrate transporter operon under *lac* promoter. Lane1- Marker HindIII, Lane2- Plasmid undigested, Lane-3 pJIYC digested with PvuII, and Lane-4 pGRG36vhb, *egfp* plasmid digested with PvuII.

B. japonicum USDA110, *M. loti* MAFF030669 and *S. fredii* NGR234 integrants were confirmed based on PCR amplification of YF-CitC from genomic DNA (**Fig. 7.4**).

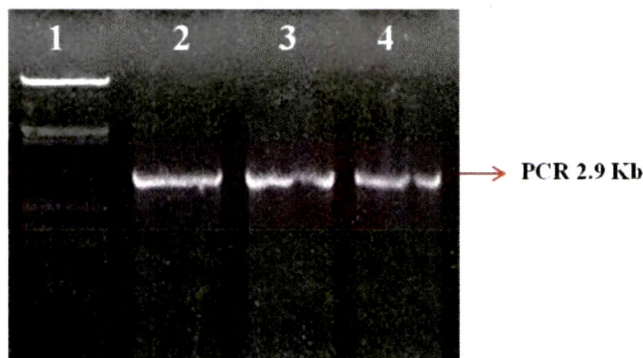


Fig. 7.4: Confirmation of Genome integrants by PCR amplification of YF-citC from *B. japonicum* USDA110 , *M. loti* MAFF030669 and *S. fredii* NGR234 integrants: Lane1- Marker HindIII/EcoRI. Lane- 2,3,4 PCR amplicon of YF-citC from genomic DNA of *B. japonicum* USDA110 , *M. loti* MAFF030669 and *S. fredii* NGR234 integrants.

7.3.2: CS activity and MPS ability of *B. japonicum* USDA110 , *M. loti* MAFF030669 and *S. fredii* NGR234 integrants on 50 mM Tris-Cl buffer pH 8 and 50 mM glucose containing rock phosphate.

The CS activity of *B. japonicum* USDA110 *M. loti* MAFF030669 and *S. fredii* NGR234 integrants grown on 50 mM Tris-Cl Buffer pH 8 and 50 mM glucose, was ~2.6, ~4.3 and ~2.2 fold higher (47.13 ± 1.04 U, 54.8 ± 1.23 U and 34.5 ± 1.02 U) in the three strains, respectively, compared to control which possessed low levels of CS activity (17.85 ± 1.14 U), (12.86 ± 0.07) and (16.02 ± 0.12 U), respectively. To check MPS ability a zone of clearance and acidification was observed on PVK and TRP plates. Maximum zone of clearance and acidification was shown by *Bj. intYc*, *Ml. intYc* and *Sf. intYc* as compared to the wild type *B. japonicum* USDA110 , *M. loti* MAFF030669 and *S. fredii* NGR234 . P-solubilizing ability of wild type *B. japonicum*, *M. loti* MAFF030669 and *S. fredii* NGR234 and its transformants varied in the order of *Sf intYc* > *Bj intYc* > *Ml intYc* > *Sf* > *Bj* = *Ml* on PVK medium after 3 days of incubation at 30°C (Fig. 7.5). The integrants of *S. fredii* NGR234, *B. japonicum* USDA110 and *M. loti* MAFF030669 showed enhanced zone of clearance as compared to the wild type. Also among the three integrants showed maximum PSI (Table 7.2).

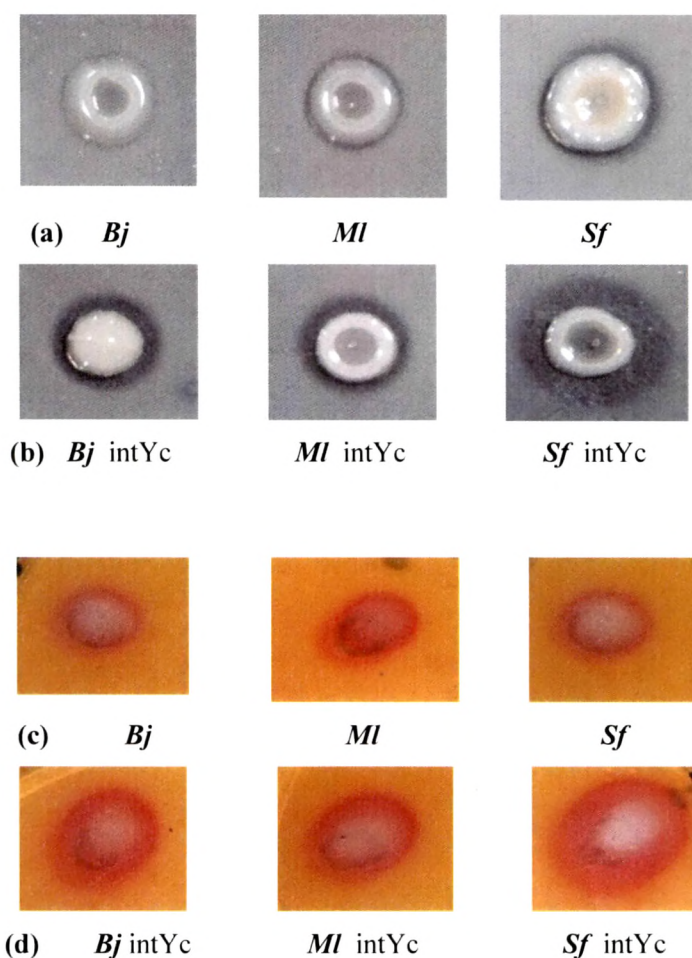


Fig. 7.5: MPS phenotype of *B. japonicum* USDA110 *M. loti* MAFF030669 and *S. fredii* NGR234 integrants (a), (b) Zone of clearance formed by *Rhizobium* integrants on Pikovskaya's agar and (c), (d) zone of acidification Tris rock phosphate agar containing 50 mM glucose and 50 mM Tris Cl buffer pH 8.0. The results were noted after an incubation of 3 days at 30 °C. Media composition and other experimental details are as described in Sections 2.2.4 and 2.7.

Table 7.2: P solubilization index on Pikovskayas agar of *B. japonicum* USDA110 , *M. loti* MAFF030669 and *S. fredii* NGR234 integrants during 3 days of growth on 50 mM Tris-Cl buffer pH 8 and 50 mM glucose containing rock phosphate. *Bj*, *Ml* and *Sf* : wild type strain; and *Bj intYc*, *Ml intYc* and *Sf intYc* : *B. japonicum* USDA110 , *M. loti* MAFF030669 and *S. fredii* NGR234 integrants. The results were noted after an incubation of 3 days at 30 °C and are given as mean ± S.D. of three independent observations as compared to native *Bj*, *Ml* and *Sf*.

<i>Rhizobium</i> Strains	Diameter of zone of clearance(mm)	Diameter of colony (mm)	Phosphate Solubilizing Index
<i>Bj</i>	12.17 ± 0.29	11.17 ± 0.29	1.09
<i>Bj.</i> intYc	13.17 ± 0.29	9.50 ± 0.50	1.44
<i>Ml</i>	12.83 ± 0.29	11.50 ± 0.50	1.09
<i>Ml.</i> intYc	14.50 ± 0.50	10.17 ± 0.29	1.40
<i>Sf</i>	12.17 ± 0.29	10.50 ± 0.50	1.20
<i>Sf.</i> intYc	16.50 ± 0.50	9.17 ± 0.29	1.78

7.3.4: Growth pattern and pH profile of *B. japonicum* USDA110, *M. loti* MAFF030669 and *S. fredii* NGR234 integrants on 50 mM Tris-Cl buffer pH 8 and 50 mM glucose containing rock phosphate.

The growth of *Bj intYc*, *Ml intYc* and *Sf intYc* on 50 mM Tris-Cl buffer pH 8 and 50mM glucose reached to a maximum of 1.8 O.D. within 12 h in integrants compared to 20 h of the native *B. japonicum* USDA110, *M. loti* MAFF030669 and *S. fredii* NGR234 strains. pH of the medium dropped to 6.8, 6.8 and 5.7 within 20 h in the native *B. japonicum* USDA110, *M. loti* MAFF030669 and *S. fredii* NGR234, while pH drop to 3.84, 4.22 and 4.31 was seen within 12 h in *B. japonicum* USDA110, *M. loti* MAFF030669 and *S. fredii* NGR234 integrants, respectively (Fig. 7.6; 7.7; 7.8).

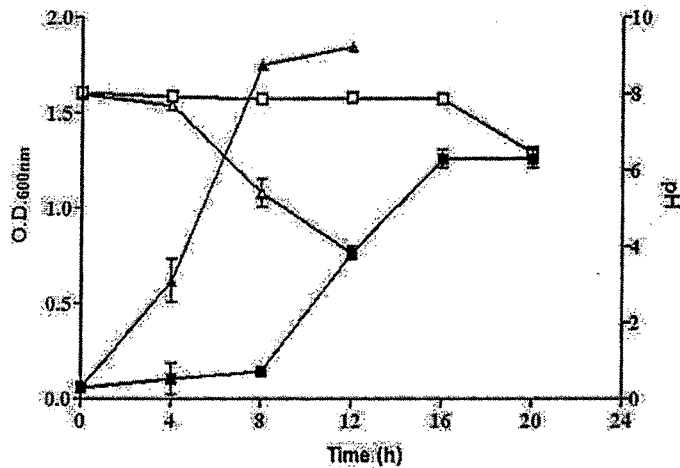


Fig. 7.6: Extracellular pH (□, Δ,) and growth profile on glucose 50 mM, Tris-Cl 50 mM rock phosphate medium (■,▲,) of *B. japonicum* USDA110 integrant containing *YFcitC*, *vhb*, *egfp*. □, ■, *Bj* (wild type); Δ, ▲, *Bj* intYc. OD₆₀₀ and pH values at each time point are represented as the mean ± SD of six independent observations.

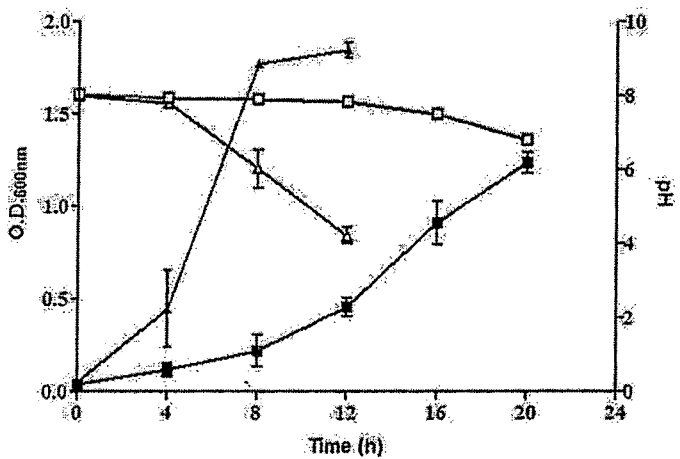


Fig. 7.7: Extracellular pH (□, Δ,) and growth profile on glucose 50 mM , Tris-Cl 50 mM rock phosphate medium (■,▲,) of *M. loti* MAFF030669 integrant containing *YFcitC*, *vgb* and *egfp*. □, ■, *Ml* (wild type); Δ, ▲, *Ml* intYc. OD₆₀₀ and pH values at each time point are represented as the mean ± SD of six independent observations.

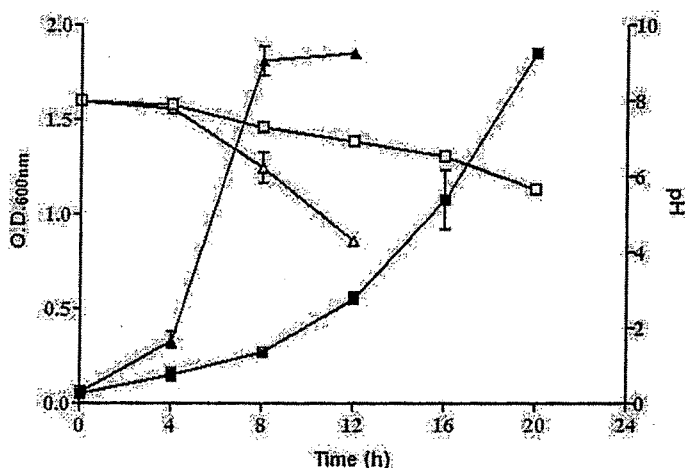


Fig.7.8: Extracellular pH (□, Δ,) and growth profile on glucose 50 mM , Tris-Cl 50 mM rock phosphate medium (■,▲,) of *S. fredii* NGR234 integrant containing *YFcitC*, *vgb*, *egfp*. □, ■, *Sf* (wild type); Δ, ▲, *Sf intYc*. OD₆₀₀ and pH values at each time point are represented as the mean ± SD of six independent observations.

7.3.5: Physiological effect of genomic integration on 50 mM Tris-Cl buffer pH 8 and 50 mM glucose containing rock phosphate.

In presence of 50 mM glucose, genomic integration showed ~1.73, ~1.72 and ~2.2 fold increase in growth profile by *Bj intYc*, *Ml intYc* and *Sf intYc*, respectively. The total glucose utilization rate at the time of pH drop remained unaffected and the total amount of glucose consumed at the time of pH drop showed ~1.15, ~1.10 and ~1.4 fold decrease in *Bj intYc*, *Ml intYc* and *Sf intYc*, respectively, and Specific Glucose utilization Rate Q_{Glc} ($g \cdot g \text{ dcw}^{-1} \cdot h^{-1}$) decreased ~1.6, ~2.1 and ~1.9 fold. Increase in enzyme activity improved the biomass yield by ~1.5, ~2.1 and ~2.1 fold in the integrants of *B. japonicum* USDA110, *M. loti* MAFF030669 and *S. fredii* NGR234, respectively, compared to native *B. japonicum*, *M. loti* MAFF030669 and *S. fredii* NGR234 (Table 7.3).

Table 7.3: Physiological variables and metabolic data of *B. japonicum* USDA110, *M. loti* MAFF030669 and *S. fredii* NGR234 integrants grown on TRP The results are expressed as Mean ± S.E.M of 6-10 independent observations. *a* Biomass yield $Y_{dcw/Glc}$, specific growth rate (*k*) and specific glucose utilization rate (Q_{Glc}) were determined from mid log phase of each experiment. *b* Total glucose utilized and glucose consumed were determined at the time of pH drop. The difference between total glucose utilized and glucose consumed is as explained in Section 2.9.3. * $P < 0.05$, ** $P < 0.01$ and *** $P < 0.001$.

<i>Rhizobium</i> Strains	Specific Growth Rate $K(h^{-1})^a$	Total Glucose Utilized (mM) ^b	Glucose Consumed (mM) ^b	Biomass Yield $Y_{dcw/Glc}$ (g/g) ^a	Specific Glucose Utilization Rate Q_{Glc} (g.g dcw ⁻¹ .h ⁻¹) ^a
<i>Bj</i>	0.186 ± 0.03	46.20 ± 0.2	38.23 ± 1.33	1.78 ± 0.14	0.14 ± 0.01
<i>Bj intYc</i>	0.321 ± 0.01***	48.28 ± 0.12	33.15 ± 0.92	2.66 ± 0.15**	0.09 ± 0.01
<i>MI</i>	0.221 ± 0.03	45.91 ± 0.64	37.07 ± 0.55	1.36 ± 0.26	0.19 ± 0.04
<i>MI intYc</i>	0.380 ± 0.01***	48.29 ± 0.15	33.56 ± 0.40	2.80 ± 0.28***	0.09 ± 0.01
<i>Sf</i>	0.260 ± 0.02	46.10 ± 0.42	37.17 ± 0.55	1.85 ± 0.1	0.15 ± 0.02
<i>Sf intYc</i>	0.569 ± 0.01***	48.26 ± 0.1	26.82 ± 1.07	3.95 ± 0.17***	0.08 ± 0.01

7.3.6: P solubilization and organic acid by *B. japonicum* USDA110, *M. loti* MAFF030669 and *S. fredii* NGR234 integrants in 50 mM Tris-Cl buffer pH 8 and 50 mM glucose containing rock phosphate.

There was significant increase in release of P by ~11.2, ~8.6 and ~11.24 fold by *Bj intYc*, *MI intYc* and *Sf intYc*, respectively, compared to wild type when grown in 50 mM Tris-Cl Buffer pH 8 containing 50 mM glucose containing Rock Phosphate 1mg/ml (Fig. 7.9).

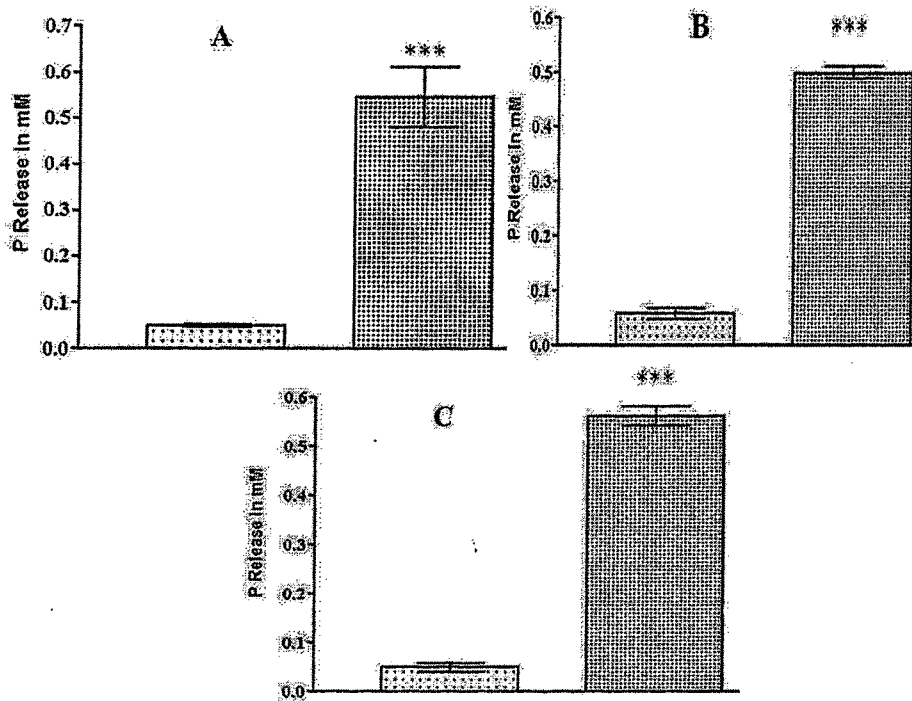


Fig. 7.9: P Solubilization by different integrants. (A)- *Bj*, *Bj intYc*, (B)- *Ml*, *Ml intYc* and (C) *Sf*, *Sf intYc*; on 50 mM Tris-Cl buffer pH 8 and 50 mM glucose containing rock phosphate. Results are expressed as Mean \pm S.E.M of 4-6 independent observations. * $P < 0.05$, ** $P < 0.01$ and *** $P < 0.001$.

On 50 mM Tris-Cl pH 8 and in presence of 50 mM glucose, the organic acids identified were mainly gluconic, 2-ketogluconic, acetic and citric acids. Extracellular medium of *Bj intYc*, *Ml intYc* and *Sf intYc* showed ~ 9.4 , ~ 9.6 and ~ 7.9 -fold increase in citric acid with specific citric acid yield $Y_{C/G}$ ~ 2.7 , ~ 3.5 and ~ 1.5 fold, respectively, which is ~ 2.1 , ~ 1.9 and ~ 2.8 - fold higher amount of gluconic acid as compared to native with specific gluconic acid yield, $Y_{G/G}$, increasing by ~ 1.7 , ~ 1.5 and ~ 1.8 fold, respectively (Fig. 7.10). There was no change in the intracellular citric acid levels. (Table

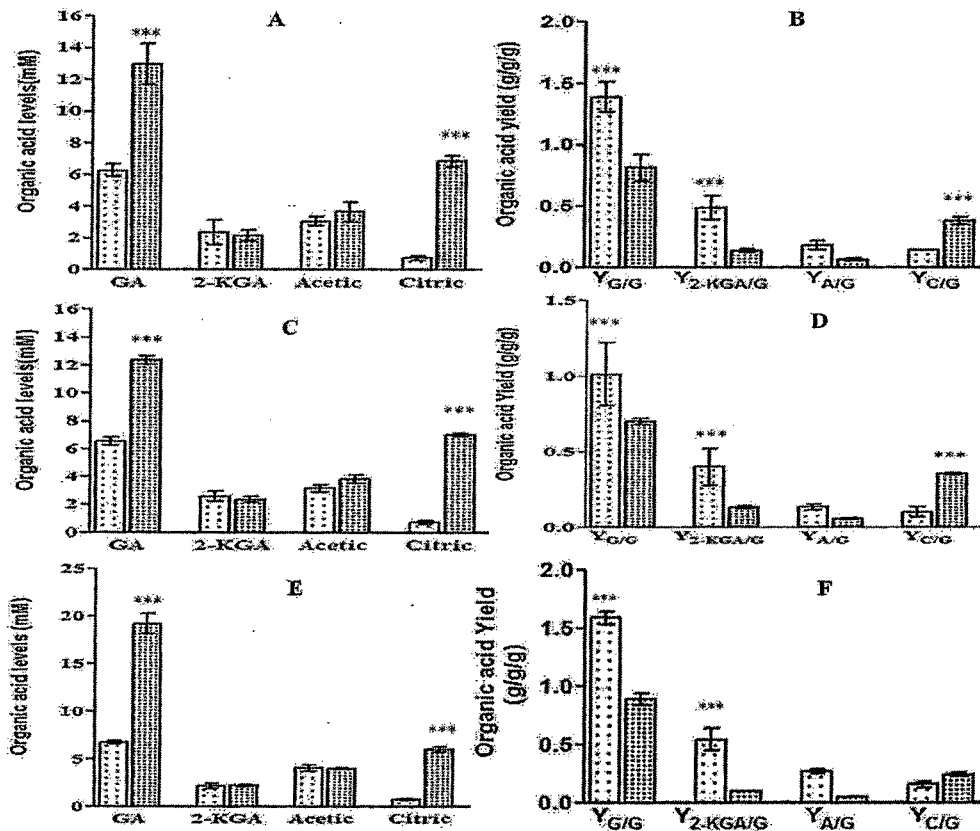


Fig.7.10: Organic acid production by three integrants. (A, B)-*Bj*, *Bj*. intYc.) (C, D)-*Ml*, *Ml*. intYc and (E, F)-*Sf*, *Sf*. intYc; (A), (C), (E) Organic acids in mM (B), (D), (E) Organic acid yields, grown on 50 mM Tris-Cl buffer pH 8 and 50 mM glucose containing rock phosphate. All organic acids are estimated from stationary phase cultures (at the time of pH drop). Results are expressed as Mean \pm S.E.M of 4-6 independent observations. * P<0.05, ** P<0.01 and *** P<0.001.

Table 7.4: Intracellular citric acid levels of *B. japonicum* USDA110, *M. loti* MAFF030669 and *S. fredii* NGR234 integrants grown on TRP.

<i>Rhizobium</i> Strains	Intracellular Citric acid in mM
<i>B.japonicum</i> USDA110	0.83 ± 0.06
<i>Bj</i> intYc	0.85 ± 0.04
<i>M. loti</i> MAFF030669	0.85 ± 0.04
<i>Ml</i> intYc	1.07 ± 0.09
<i>S. fredii</i> NGR234	1.48 ± 0.08
<i>Sf</i> intYc	1.32 ± 0.31

7.3.7: Alterations in enzyme activities in *B. japonicum* USDA110 *M. loti* MAFF030669 and *S. fredii* NGR234 integrants .

Genome integrants were further analyzed for alterations in physiological variables and organic acid profile, enzymes involved periplasmic direct oxidation and intracellular phosphorylative pathways. There was an overall increase in all the enzyme activities. **GDH** activity increased by about ~1.95, ~1.3 and ~2.1- fold; **PPC** activity increased by ~1.7, ~1.3-fold and no change; **PYC** increased by ~2.6, ~2.5 and ~2.0-fold; **CS** increased by ~2.6, ~4.3 and ~2.2-fold; **ICL** increased by ~1.5, ~1.3-fold and no change, **ICDH** increased by ~1.5, ~1.8 and ~1.6-fold and **G-6-PDH** increased by ~1.6, ~1.4 and ~1.5-fold in *Bj. intYc*, *Ml. intYc* and *Sf. intYc* or *B. japonicum* USDA110 *M. loti* MAFF030669 and *S. fredii* NGR234 integrants respectively compared to the native strains (Fig. 7.11,7.12 and 7.13).

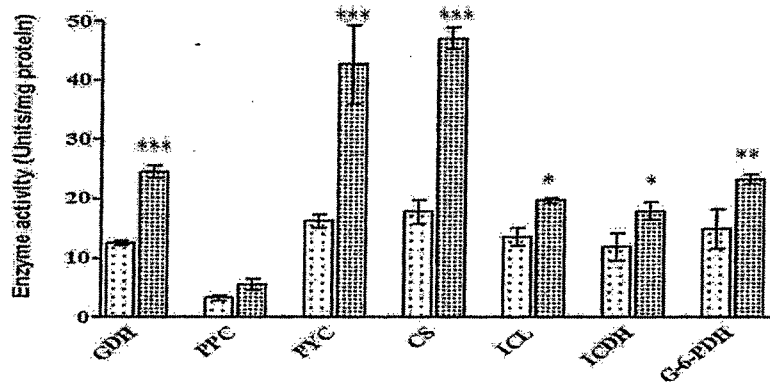


Fig.7.11: Alterations in enzyme activities in *B. japonicum* USDA110 integrants (▨, *Bj*; ▩, *Bj.intYc*). The activities have been estimated using cultures grown on M9 minimal medium with 50 mM glucose. All the enzyme activities are represented in the units of nmoles/min/mg total protein. Results are expressed as Mean ± S.E.M of 4-6 independent observations. * P<0.05, ** P<0.01 and *** P<0.001.

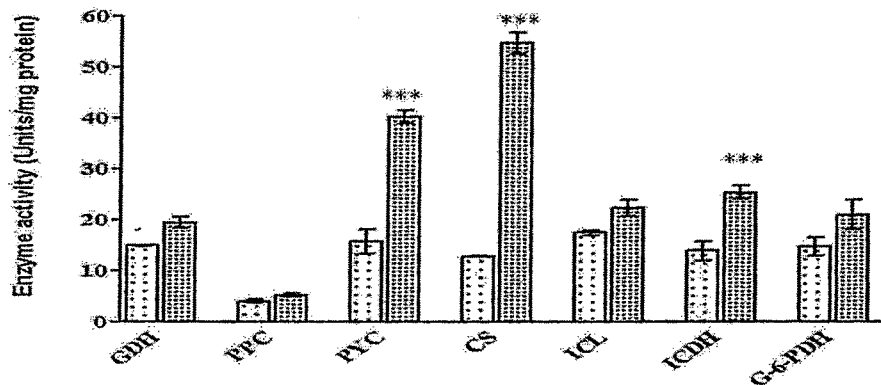


Fig. 7.12: Alterations in enzyme activities in *M. loti* MAFF030669 integrants (▨, *Ml*; ▩, *Ml.intYc*). The activities have been estimated using cultures grown on M9 minimal medium with 50 mM glucose. All the enzyme activities are represented in the units of nmoles/min/mg total protein. Results are expressed as Mean ± S.E.M of 4-6 independent observations. * P<0.05, ** P<0.01 and *** P<0.001.

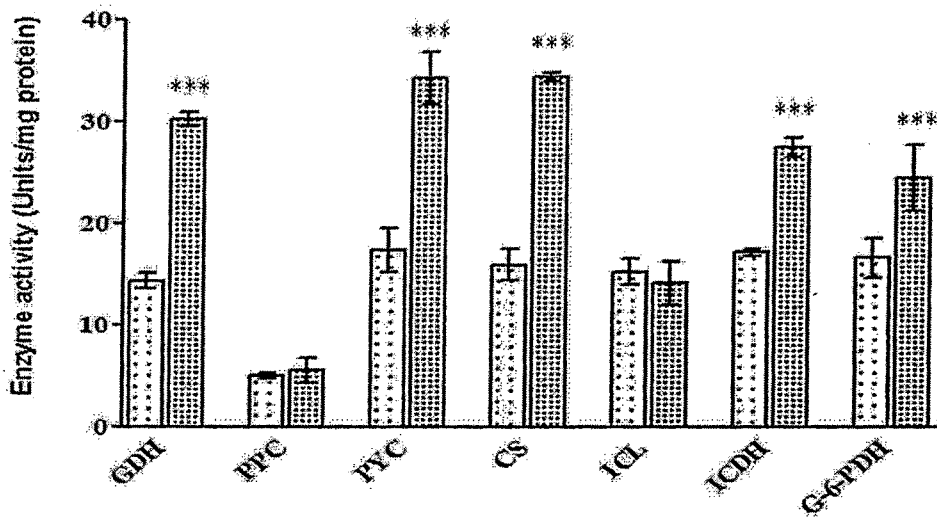


Fig. 7.13: Alterations in enzyme activities in *S. fredii* NGR234 integrants (□, *Sf.*; ▨, *Sf. intYc.*). The activities have been estimated using cultures grown on M9 minimal medium with 50 mM glucose. All the enzyme activities are represented in the units of nmoles/min/mg total protein. Results are expressed as Mean ± S.E.M of 4-6 independent observations. * P<0.05, ** P<0.01 and *** P<0.001.

7.4: DISCUSSION

Genetic engineering of microorganisms involves the use of extra-chromosomal plasmid for heterologous expression of desired genes. Plasmid DNA is known to cause metabolic burden on the cell and alter its metabolism depending on the host organism, plasmid nature, and environmental conditions (Buch et al., 2010b; Sharma et al., 2011). Hence, genetic manipulations need to be directed towards chromosomal integration as it would lead not only to increased stability but also decrease the metabolic load caused by the presence of the plasmids to nullify the pleiotropic effects on the host metabolism. The present study demonstrates the effect of genomic integration of *E. coli* NADH insensitive *cs* Y145F gene and *S. typhimurium* *citC* gene on *B. japonicum* USDA110, *M. loti* MAFF030669 and *S. fredii* NGR234.

In our study, genomic integrants of *B. japonicum*, *M. loti* MAFF030669 and *S. fredii* NGR234 showed MPS phenotype in 50 mM Tris pH 8.0 while corresponding plasmid transformants showed phenotype even on 100 mM Tris pH 8.0 medium. Hence, the strength acidification by the genomic integrants had decreased. This was contrary to the phenotype expected on the basis of metabolic load between plasmid transformants and genomic integrants. This, it appears that the higher level overexpression of genes in plasmid transformants, due to high copy number of the genes, may be responsible for their better MPS phenotype.

The metabolic differences among the various transformants and the integrants may be due to the differences in the copy numbers, the former having 10-16 plasmid copy number. Plasmid nature and copy number are known to exert load on cellular physiology leading to significant alterations in the metabolism (Schweder et al, 2002; Wang et al., 2006; De Gelder, 2007). The copy number of the plasmids used in this study (pAB4, pAB3, pAB8, pAB7) in *P. fluorescens* 13525 was found to be 10-16 and was independent of the nature of antibiotic resistance.(Buch et al., 2010) The increased phenotype in plasmid transformants is due to high copy number of plasmids, so more

overexpression, and more enzyme activity resulted in increased amount of acid. While in the integrants, single copy number produced less amount of acid, and thus showed decreased phenotype compared to transformants. Here metabolic load is not so high in the laboratory conditions compared to copy number effect.

There was significant increase in activities of GDH, G-6-PDH, PPC, PYC, CS, ICL and ICDH in integrants of all the three strains, suggesting increase in oxidative and phosphorylative pathway and higher flux of glucose through TCA in *Rhizobium* leading to increase in gluconic acid and citric acid (Fuhrer, 2005). In addition to the metabolic alterations in the central carbon pathway, this work also deals with the overexpression of *vgb* gene in *Rhizobium* spp. along with artificial citrate operon to improve the recombinant protein production and better survival of host under microaerobic conditions (Frey and Kallio, 2003). A loss of MPS ability under low aeration conditions was seen in case of *Citrobacter* sp. DHRSS containing citrate operon with a concomitant loss of citric and gluconic acid secretion. Presence of *vgb* gene restored the citric and gluconic acid secretion along with MPS ability under microaerobic conditions (Yadav, 2013). In this study *vgb* effect was seen under aerobic condition and effect in microaerobic condition is yet to be investigated.

The genetically modified strains are expected to be an efficient phosphate solubilizing bacterium (PSB) in rhizosphere soil. This paves the way for genetic modification of other plant growth promoting rhizobacteria to enable them to secrete higher amount citric acid and converting into efficient PSB.